**Supplementary Information**

**for**

# Copper-β-amyloid peptides exhibit neither monooxygenase nor superoxide dismutase activities

**Davide Ciregna, Enrico Monzani, Grégory Thiabaud, Silvia Pizzocaro, and Luigi Casella***

Dipartimento di Chimica, Università di Pavia, 27100 Pavia, Italy.

## 1. General Methods

The synthesis of Aβ16 and Aβ28 peptides was carried out by solid phase synthesis with Fmoc chemistry. After removal of the peptide from the resin and deprotection, the crude products were purified by RP HPLC on a Supelcosil$^{TM}$ LC18 column, using a Jasco MD-1510 instrument with diode array detection. The purified peptides were lyophilized and stored at -20 °C until use. The identity of the peptides was confirmed by one and two-dimensional ($^{1}$H-$^{1}$H DQF-COSY) NMR (Bruker AVANCE 400) and by EI-MS (Thermo-Finnigan). HFIP treatment was carried out upon lyophilization of the peptide after dissolution in HFIP.[1S] The concentration of Aβ peptides in solution was based on UV measurements at 280 nm using the extinction coefficient of the tyrosine residue (1280 $M^{-1}$ $cm^{-1}$).[2S,3S] Kinetic experiments were performed on a HP 8453 spectrophotometer and monitored between 200 and 800 nm using a quartz cuvette with magnetic stirring and 1 cm path length.

## 2. Catalytic Oxidations

Phenol hydroxylation and catechol oxidation experiments with [$Cu^{II}$-Aβ16] or [$Cu^{II}$-Aβ28] were carried out by reacting equimolar concentrations of phenol, or catechol, and MBTH (typically from

0.1 to 1.0 mM) in HEPES buffer at pH 7.0 in the presence of the $Cu^{II}$-Aβ complex (typically from 2.5 to 25 μM). The phenol hydroxylation experiments were repeated using copper(II) nitrate and variable amounts of Aβ peptide. The formation of the red adduct between the quinone product and MBTH was monitored at 500 nm ($\varepsilon = 32500\ M^{-1}\ cm^{-1}$). Identical results were obtained using freshly prepared $Cu^{II}$-Aβ solutions or preincubating the solutions for 0.5 h before performing the oxidation reactions. The oxidation of phenol or catechol was not observed when the reaction was performed under anaerobic conditions. Blank experiments on the autoxidation of phenol and catechol under the same conditions but in the absence of [$Cu^{II}$-Aβ] complex were found to be completely negligible even after 24 h. Control experiments using HFIP-treated Aβ peptides are described in paragraph **4**. Standard samples of the MBTH-p-quinone and MBTH-o-quinone adducts were prepared on a larger scale to enable the identification of the type of quinone involved and will be described in detail in paragraph **6**.

### 3. CD spectra of HFIP-treated Aβ16 and Aβ28, and their copper(II) complexes

The CD spectra of Aβ16 and Aβ28 peptides, in 1 mM HEPES buffer, pH 7.0, before and after treatment with HFIP are reported in Figure 1S and 2S.

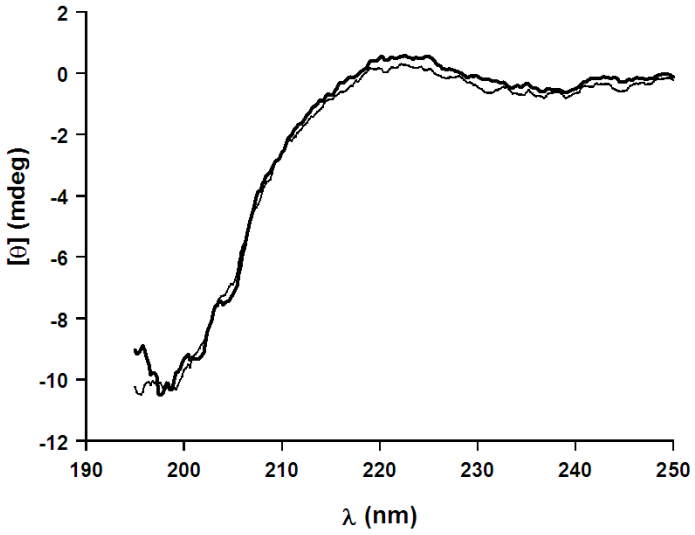


**Figure 1S**. CD curves of Aβ16 (0.1 mM, path length 0.1 cm) before (thick line) and after (thin line) treatment with HFIP. Three rapid scans (50 nm/min) were accumulated to prevent eventual aggregation of the freshly dissolved HFIP-treated peptide.


**Figure 2S**. CD curves of Aβ28 (0.05 mM, path length 0.1 cm) before (thick line) and after (thin line) treatment with HFIP. Three rapid scans (50 nm/min) were accumulated to prevent eventual aggregation of the freshly dissolved HFIP-treated peptide.

The CD spectra of Aβ16 and Aβ28 (untreated samples), in 1 mM HEPES buffer, pH 7.0, are compared with those of the corresponding copper(II) complexes in Figures 3S and 4S. The spectra of HFIP-treated derivatives are identical.

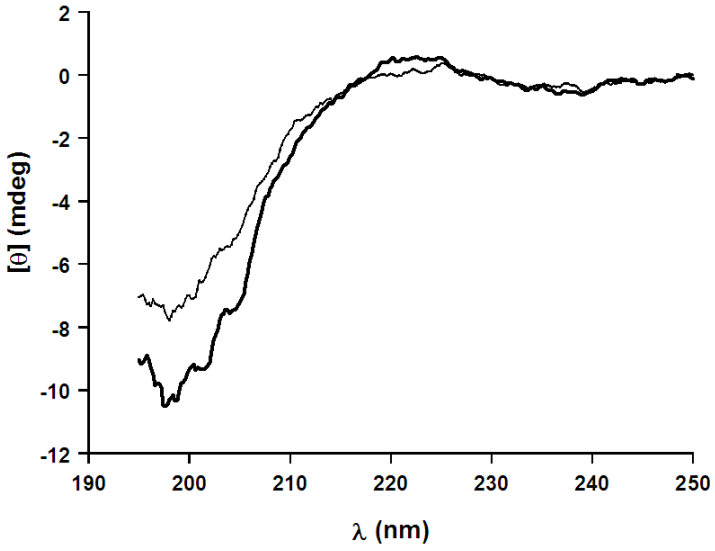


**Figure 3S**. CD curves (three rapid scans) of Aβ16 (0.1 mM, thick line) and [$Cu^{II}$-Aβ16] (0.1 mM, thin line).

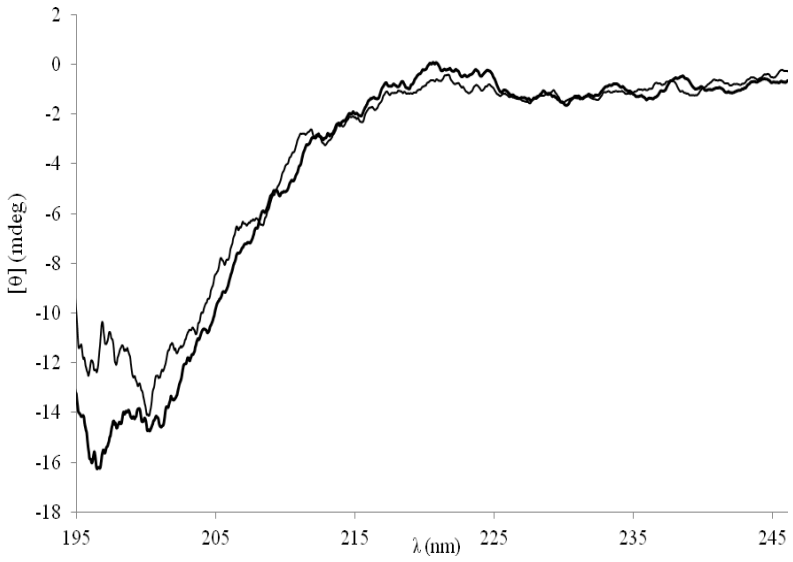


**Figure 4S**. CD curves (three rapid scans) of Aβ28 (0.05 mM, thick line) and [$Cu^{II}$-Aβ28] (0.05 mM, thin line).

## 4. Catalytic oxidation of phenol in the presence of MBTH, copper(II) and HFIP-treated Aβ16 or Aβ28 - Effect of the copper(II)/peptide ratio

*a. With Aβ16*

The experiments were performed in 100 mM HEPES buffer at pH 7.0 equilibrated with atmospheric oxygen and containing 1 mM phenol and 1 mM MBTH. The reactions started upon adding the peptide (in variable amount) followed by copper(II) nitrate (2.5 μM) as the last reagent. The aggregate-free peptide, from 0.0 to 1.0 equiv., was added as a freshly prepared solution obtained from HFIP-treated Aβ16 peptide. The reactions were performed in a thermostated optical cell equipped with a magnetic stirrer. The kinetic traces of the reactions, obtained by monitoring the band of the red adduct between the quinone product and MBTH at 500 nm, show the progressive inhibitory effect exerted by Aβ16 (Figure 5S). With 2.0 equiv. Aβ16 the reaction was totally bleached (data not shown).

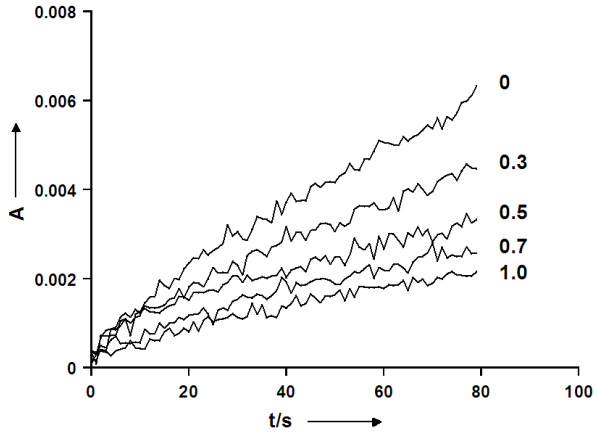


**Figure 5S.** Representative kinetic traces in the initial phase of the reaction (after the mixing time) for the formation of the MBTH-quinone adduct by oxidation of phenol (1 mM) in the presence of MBTH (1 mM), $Cu^{2+}$ (2.5 μM) and variable amounts of HFIP-treated Aβ16 (0, 0.2, 0.5, and 1.0 equiv.), in HEPES buffer (100 mM) at pH 7.0.

*b. With Aβ28*

The experiments were performed as described above for Aβ16. The reactions started upon adding the peptide (in variable amount) followed by copper(II) nitrate (5.0 μM) as the last reagent. The aggregate-free peptide was added as a freshly prepared solution obtained from HFIP-treated Aβ28. The reactions were performed in a thermostated optical cell equipped with a magnetic stirrer. The kinetic traces of the reactions, obtained by monitoring the band of the red adduct between the quinone product and MBTH at 500 nm, show the progressive inhibitory effect exerted by Aβ28 (Figure 6S). With 2.0 equiv. Aβ28 the reaction was totally bleached (data not shown).

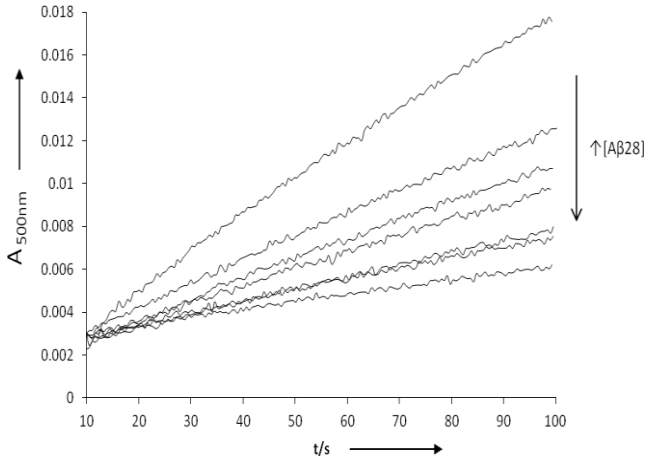


**Figure 6S.** Representative kinetic traces in the initial phase of the reaction (after the mixing time) for the formation of the MBTH-quinone adduct by oxidation of phenol (1 mM) in the presence of MBTH (1 mM), $Cu^{2+}$ (5.0 μM) and increasing amounts of HFIP-treated Aβ28 (from top to bottom: 0.0, 0.2, 0.3, 0.4, 0.6, 0.7, and 1.0 equiv.), in HEPES buffer (50 mM) at pH 7.0.

## 5. Reduction of [$Cu^{II}$-Aβ16] by MBTH under anaerobic conditions

The experiment was performed in an optical cell equipped with Schlenk connections. A 0.6 mM solution of [$Cu^{II}$-Aβ16] (or the corresponding copper complex prepared from HFIP-treated Aβ16) in 100 mM HEPES buffer at pH 7.0 was carefully degassed through several vacuum/argon cycles. Then, a concentrated and degassed methanol/buffer (50 % v/v) solution of MBTH (1 mM final concentration) was added with a gas-tight syringe. The complete bleaching of the visible absorption of the copper(II) complex occurred within a few minutes. No reaction occurs when the catalytic experiments of phenol oxidation described in paragraph **2** are performed under anaerobic conditions.

## 6. Characterization of MBTH-Quinone Adducts Derived from Phenol

*a. Reaction of phenol with MBTH and $Cu^{2+}$ salt*

In this experiment, phenol (20 mg, 0.11 M) and MBTH (40 mg, 0.09 M ) were dissolved in water (2 ml) in the presence of a catalytic amount of $Cu(NO_3)_2$ ($10^{-4}$ M). The solution was allowed to react at room temperature for about 5 min and then it was extracted with $CHCl_3$ (3×2 ml). The combined

organic fraction was dried over $MgSO_4$, filtered and the solvent was removed by rotary evaporation. The resulting crude product was dissolved in a mixture of $CH_2Cl_2$/MeOH 97:3 (v/v) and chromatographed on a $SiO_2$ column. The eluted fraction was rotary evaporated, and the red addition product characterized by ESI-MS (molecular peak at 270 amu) and $^1$H-NMR (DMSO-$d_6$ solution); the NMR spectrum of this product is shown in Figure 7S(a). The assignment of the peaks was made through $^1$H and $^1$H-$^1$H DQF-COSY experiments. The peaks near 6.8 e 7.2 ppm are due to unreacted phenol that coeluted with the product.

*b. Reaction of para-quinone with MBTH and $Cu^{2+}$ salt*

The standard of MBTH-*para*-quinone adduct was obtained by reacting a solution of *p*-quinone (20 mg, 0.09 M), MBTH (40 mg, 0.09 M), and $Cu(NO_3)_2$ ($10^{-4}$ M) in water (2 ml) for 2 min, followed by workup as described above. The $^1$H NMR spectrum of the resulting MBTH-*para*-quinone adduct in DMSO-$d_6$ is shown in Figure 7S(b).

*c. Reaction of phenol with MBTH and tyrosinase*

The standard MBTH-*ortho*-quinone adduct was prepared by enzymatic oxidation of phenol (20 mg, 0.11 M) with tyrosinase (~ $10^{-8}$ M) in aqueous phosphate buffer pH 7.0 for 2 min, after which MBTH (40 mg, 0.09 M) was added. The condensation product was then isolated through the usual procedure. The $^1$H NMR spectrum of the MBTH-*ortho*-quinone adduct in DMSO-$d_6$ is shown in Figure 7S(c).

**Figure 7S**. Proton NMR spectra of the MBTH-quinone adducts recorded in DMSO-$d_6$.

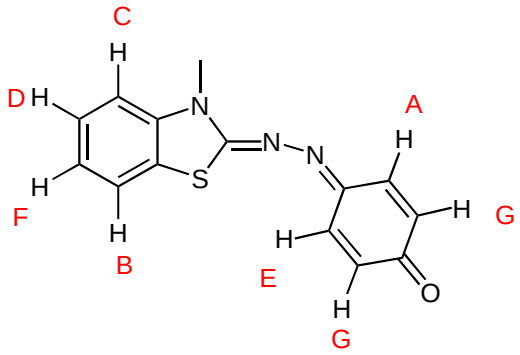


c)

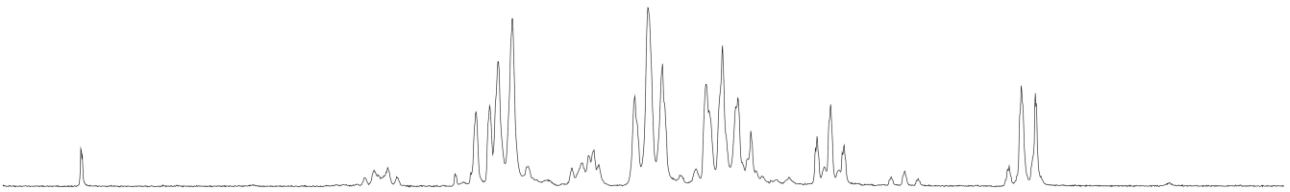

b)

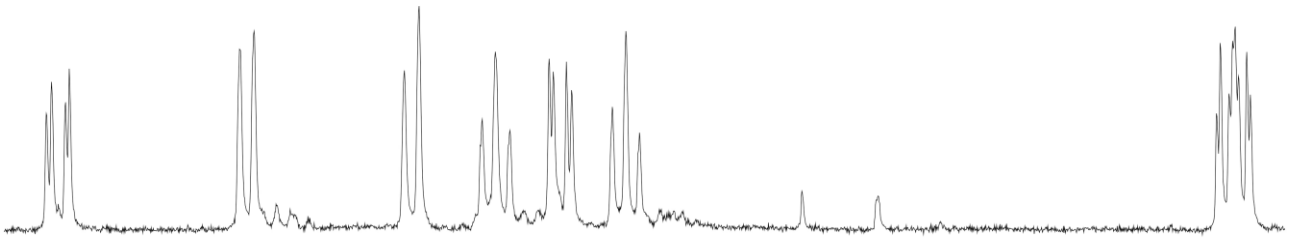

a)

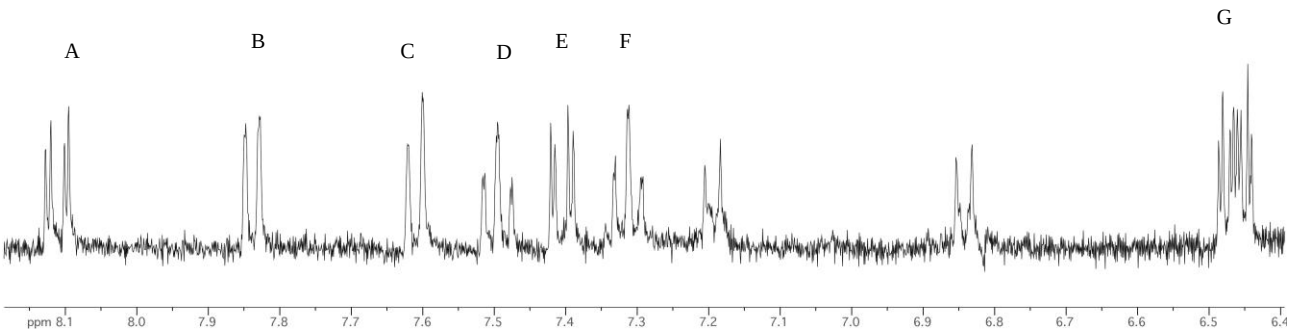

## 7. Catalytic oxidation of 4-methylcatechol in the presence of MBTH, copper(II) and Aβ28 - Effect of the copper(II)/peptide ratio

The experiments were performed in 50 mM HEPES buffer at pH 7.0 equilibrated with atmospheric oxygen, or pure oxygen, and containing 0.1 mM 4-methylcatechol and 0.1 mM MBTH. The reactions started upon adding the peptide (in variable amount) and copper(II) nitrate (25 μM). The peptide, from 0.0 to 1.6 equiv., was added as a freshly prepared solution obtained from lyophilized Aβ28. The reactions were performed in a thermostated optical cell equipped with a magnetic stirrer. The kinetic traces of the reactions were obtained by monitoring the absorbance at 500 nm.

*a. Effect of Aβ28 in the catalytic oxidation of 4-methylcatechol*

As reported in the text, the kinetic trace of the copper(II) catalytic oxidation of 4-methylcatechol is affected by the presence of Aβ28 (Figure 2). While the reaction profile exhibited by free copper(II) is linear, a biphasic behaviour is observed in the presence of Aβ28, with a fast initial phase followed by a slower, linear phase. The absorbance change in the first step is proportional to the copper(II) concentration, indicating a stoichiometric phase, while the second phase is catalytic. Increasing [Aβ28], the slope of the first phase gradually increases while that of the catalytic phase decreases (data not shown).

*b. Effect of the molecular oxygen concentration*

The reactions were studied both in buffer solution saturated with atmospheric oxygen and with pure oxygen at 1 atm. In the absence of Aβ28, the copper(II) catalyzed reaction exhibits a linear absorbance vs. time profile, with a slope undergoing a marked increase passing from air to pure oxygen (Figure 8S). On the other hand, in the presence of 1 equiv. of Aβ28, the reaction profiles are biphasic and an increase of oxygen concentration produces an increase in the slope of the catalytic phase but does not affect the slope of the initial phase involving copper(II) reduction (Figure 9S).

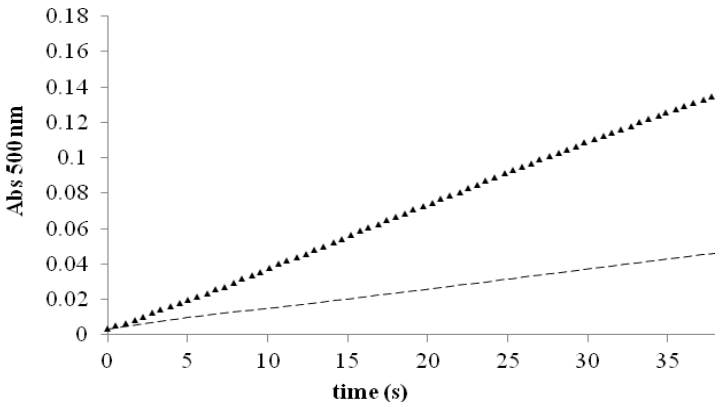


**Figure 8S**. Kinetic traces in the initial phase of the reaction (after the mixing time) for the oxidation of 4-methylcatechol (0.1 mM) in the presence of MBTH (0.1 mM) and $Cu^{2+}$ (25 μM), in 50 mM HEPES buffer at pH 7.0 saturated with air (dashed line) or pure oxygen (triangles).

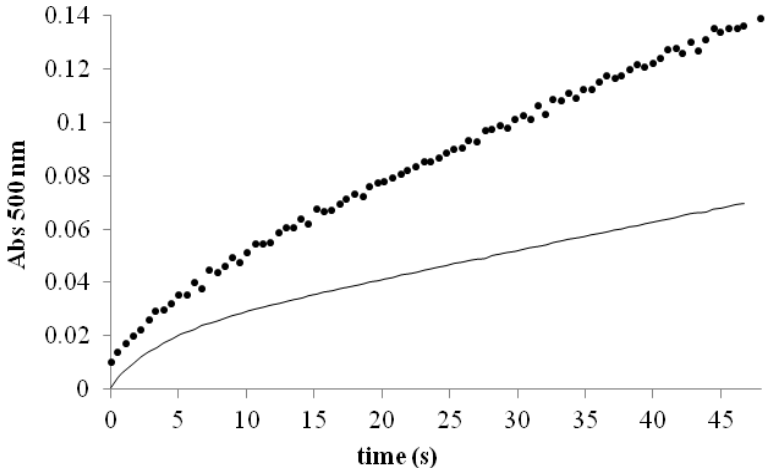


**Figure 9S**. Kinetic traces in the initial phase of the reaction (after the mixing time) for the oxidation of 4-methylcatechol (0.1 mM) in the presence of MBTH (0.1 mM), $Cu^{2+}$ (25 μM), and HFIP-treated Aβ28 (1.0 equiv.), in HEPES buffer (50 mM) at pH 7.0 saturated with air (full line) or pure oxygen (dotted line).

*c. Kinetic mechanism and fitting of the data*

The kinetic profile exhibited by free copper(II) in the oxidation of 4-methylcatechol in the presence of MBTH is linear with a rate depending both on copper and dioxygen concentrations in the buffer. This is consistent with a rate determining step that does not change during the reading of the absorbance data. A different behaviour is observed when the reaction is carried out in the presence

of Aβ28. In this case, an initial fast phase, lasting a few seconds, and stoichiometric (with respect of copper) is followed by the slower turnover of the catalyst giving the linear part of the absorbance vs. time profile. The first phase is independent of $[O_2]$, while the turnover rate depends on that. This indicates that the rate determining step of the turnover rate, both in the absence or presence of the peptide, is connected with the formation of a Cu-$O_2$ intermediate. The fast initial phase observed in the presence of peptide is due to the fact that the catalysis starts with the reaction of [$Cu^{II}$-Aβ28] with the metal in the oxidized form. Then, the copper(II) ion undergoes a fast reduction by MBTH, giving rise to the radical cation $MBTH^{\bullet+}$ which evolves to chromophoric species responsible for the initial absorbance changes. Then, the copper(I) species reacts with molecular oxygen in the rate determining step of the cycle, giving rise to an active species capable to oxidize the catechol to quinone, according to the following reactions:

*1 Step*: $Cu^{II} + MBTH \rightarrow\rightarrow Cu^{I} + MBTH^{\bullet+}$ ($k_{1obs}$)

*2 Step*: $Cu^{I} + O_2 + catechol \rightarrow\rightarrow Cu^{II} + H_2O + quinone$ ($k_{2obs}$)

It should be noted that each step could be seen as an ensemble of reactions since they involve the reversible binding of the metal ion to the peptide, the production of $MBTH^{\bullet+}$ (whose decomposition products contribute to the absorbance changes), the formation of the semiquinone radical, its dismutation to quinone and catechol, and the reaction of the quinone with MBTH finally yielding the species which is spectrophotometrically detected.

The kinetic treatment of this reaction scheme was previously described in a paper from our group.[5S] The absorbance profile can be fitted with the following rate equation, describing the development with time of the MBTH-quinone species (P) as a function of the initial copper(II) concentration ($[A_0]$). The constants $k_{1obs}$ and $k_{2obs}$ are the observed first order rate constants describing the first step (reduction of copper(II)) and the second step (formation of the active species upon reaction with $O_2$) of the catalytic cycle, respectively.

$$[P] = \frac{k_{obs1} \times [A_0]}{k_{obs1} + k_{obs2}} \times \left\{ 2 \cdot k_{obs1} \times t + \frac{k_{obs1} - k_{obs2}}{k_{obs1} + k_{obs2}} \times \left[ 1 - \exp\left[ -\left( k_{obs1} + k_{obs2} \right) \times t \right] \right] \right\} \qquad (1)$$

Fitting of the absorbance vs. time data at different Aβ28/copper(II) ratios allows the determination of the rate constants $k_{1obs}$ and $k_{2obs}$ describing the kinetic traces. Figure 10S shows the peptide/Cu molar ratio dependence of the two observed rate constants.

The observed rate constants describing the two steps are oppositely influenced by the Aβ28/Cu ratio. As this ratio increases, the $k_{1obs}$ rate constant increases, while the $k_{2obs}$ rate constant decreases, up to a saturation behaviour, showing the subtle role exerted by the peptide. The data indicate that

the coordination of Aβ28 peptide to the copper ion facilitates its reduction by the reducing agents in solution (MBTH) and slows down the formation of the Cu-$O_2$ active intermediate, probably by stabilising the reduced, copper(I), form of the metal ion.

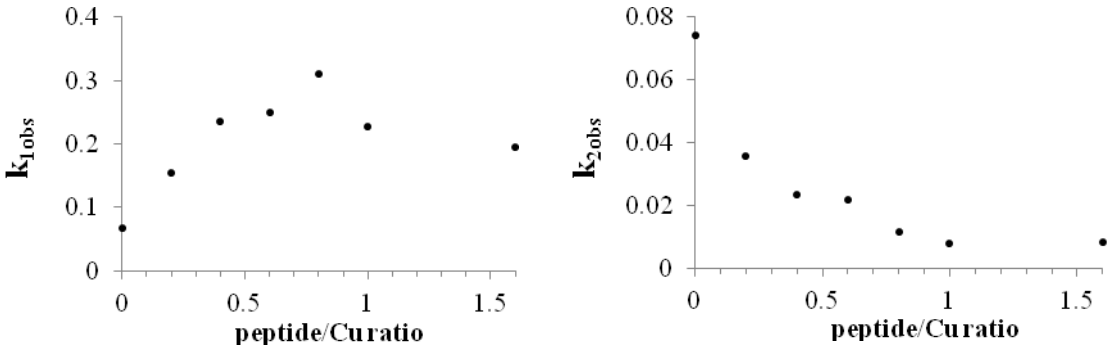


**Figure 10S**. Dependence on the Aβ28/Cu molar ratio of the observed first order rate constants $k_{1obs}$ and $k_{2obs}$, obtained by fitting with equation 1 the rate data of oxidation of 4-methylcatechol. The value in the absence of peptide is less significant since equation 1 cannot properly fit the linear absorbance trace observed in the presence of free copper(II).

## 8. Assays to determine the SOD activity

*a. Direct methods.*

There are two main direct methods to evaluate the SOD-like activity of metal complexes. The first one consists in the generation of a known concentration of superoxide by pulse radiolysis of water and the second in the addition of a known amount of a solution of $KO_2$ (usually dissolved in DMSO in the presence of crown ethers); the superoxide dismutase activity is determined by UV-Vis monitoring the decrease of the characteristic band of superoxide in the presence of the metal complex. When the SOD activity of the complex is high, the self dismutation of superoxide can be neglected due to its low second-order rate constant ($10^5$ $M^{-1}$ $s^{-1}$)[6S] and the superoxide low concentration. The catalyzed superoxide degradation follows an observed pseudo-first order decay with a rate constant, $k_{obs}$, which depends linearly on the concentration of the metal complex. Thus, dividing $k_{obs}$ by the catalyst concentration, the second-order rate constant for the SOD-like catalyst activity, $k_{cat}$, can be obtained. This behaviour is in agreement with the following rate equation for superoxide dismutation:

$$\text{rate} = k_{cat} \times [O_2^-] \times [\text{catalyst}] \qquad (2)$$

The drawbacks of these methods are, in the first case, the need of electron pulses to afford radiolysis of water and the presence of formiate anion (required for the formation of superoxide) which could interfere with the catalyst, and in the second case, the addition of a solution of $KO_2$ in DMSO, that may also affect the rate of superoxide decomposition or alter the catalyst properties.

An alternative and more generally used method, which has been followed also in the present investigation, involves the indirect evaluation of the SOD-like activity through the so called xanthine/xanthine oxidase/nitro blue tetrazolium method. The enzyme xanthine oxidase (XAO) reacts with xanthine (XA) producing a constant flow of superoxide. Then, the anion reacts with nitro blue tetrazolium (NBT) reducing it to monoformazan ($MF^+$), the accumulation of which can be easily followed by UV-Vis in solution. The enzyme concentration to be used in the assay must be optimized in order to have a linear increase in the $MF^+$ absorbance with time; this warrants that no accumulation of superoxide occurs in solution but its concentration remains stationary to a value depending on the rate of its formation by the enzyme and that for its oxidation by NBT. When the catalyst with SOD-like activity is added to the solution, it competes with NBT for the reaction with superoxide, with a reduction in the $MF^+$ formation rate. The concentration of the catalyst which causes a reduction to a half of the $MF^+$ formation rate gives the $IC_{50}$. At this concentration the rate of the reaction between superoxide and the catalyst equals that of the anion with NBT. An active catalyst efficiently competes with NBT in the reaction with superoxide and shows a low $IC_{50}$ value. SOD activity assays of this type for [$Cu^{II}$-Aβ16] were performed following the procedures described in ref. 4S.

The weak point of the XA/XAO/NBT method is that it must be assured that the effect of the catalyst on the $MF^+$ formation rate is only connected to the complex activity in the superoxide dismutation, i.e. that the catalyst does not interfere with the xanthine oxidase activity or with the reaction between superoxide and NBT. A further point to be considered is that superoxide dismutation generates hydrogen peroxide; this is an oxidant that may be further activated by reaction with the metal complex and react with NBT, $MF^+$ or superoxide itself, thus altering the data. In order to compare the efficiency in the SOD-like activity of a metal complex obtained with the direct and indirect methods, the $IC_{50}$ values must be converted into second order rate constants.

*b. Preparation of the solution of $KO_2$/18-crown-6 in DMSO.*[7S]

A solution of $2.4\times10^{-4}$ mol of 18-crown-6 was prepared in anhydrous DMSO (3 ml). The solution was kept under argon for two days on molecular sieves 4 Å before the addition of $4.2\times10^{-5}$ mol of $KO_2$. The yellow solution was sonicated for a few minutes and then immediately used for SOD-like activity test.

*c. Measurements of SOD activities.*[8S]

Solutions of [$Cu^{II}$-Aβ16] ($2.3\times10^{-5}$ M) were prepared by mixing Aβ16 with 0.9 equiv. of $Cu^{II}(NO_3)_2(H_2O)_3$ in water (milli-Q), for 30 min under stirring. The required volume of this solution was collected and added to a 50 mM phosphate buffer solution, pH 7.4. After a few min, $2\times10^{-7}$ mol of NBT (in PBS) were added to the complex solution. Then, 30 µL ($4\times10^{-7}$ mol, estimated assuming negligible degradation of $O_2^-$ in DMSO) of the solution of $KO_2$/18-crown-6 complex in DMSO were added to the [$Cu^{II}$-Aβ16]/NBT solution, that was simultaneously and vigorously vortexed in order to homogenize the reaction. The resulting solution was then analyzed by UV-visible absorption, reading the absorbance at 560 nm (Figure 11S). The experiments were repeated for the same range of $Cu^{II}$ concentrations in the absence of Aβ16.

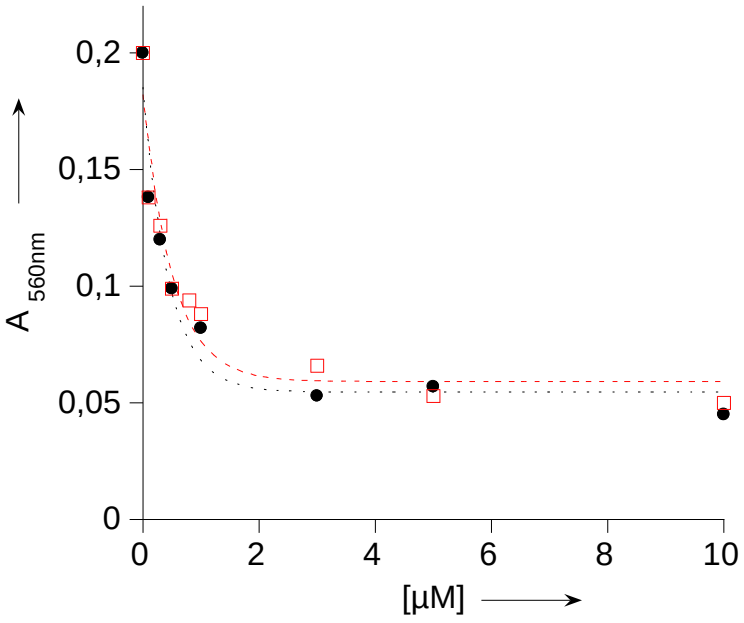


**Figure 11S**. Plots of UV-vis readings at 560 nm (50 mM aqueous phosphate buffer, pH 7.4, 300 K) for the NBT reduction (to monoformazan $MF^+$) by $O_2^-$, produced by reaction with $KO_2$/18-crown-6 in the presence of $Cu^{II}$ (black circles) or [$Cu^{II}$-Aβ16] (red squares).

Similar SOD activity experiments were performed using [$Cu^{II}$-Aβ28], the data are shown in Figure 12S.

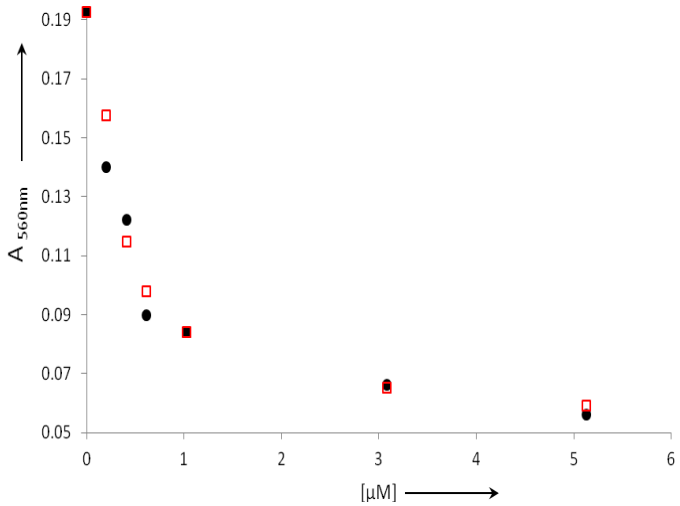


**Figure 12S**. Plots of UV-vis readings at 560 nm (50 mM aqueous phosphate buffer, pH 7.4, 300 K) for the NBT reduction (to monoformazan $MF^+$) by $O_2^-$, produced by reaction with $KO_2$/18-crown-6 in the presence of $Cu^{II}$ (black circles) or [$Cu^{II}$-Aβ28] (red squares).

## 8. References

1S. K. Broersen, W. Jonckheere, J. Rozenski, A. Vandersteen, K. Puwels, A. Pastore, F. Rousseau and J. Schymkowitz, Protein. Eng. Des. Sel. 2011, **24**, 743.

2S. R. Baruch-Suchodolsky, B. Fischer, Biochemistry 2008, **47**, 7796; ibid. 2009, **48**, 4354.

3S. S. C. Gill, P. H. von Hippel, Anal. Biochem. 1989, **182**, 319.

4S. R. Cejudo-Marin, G. Alzuet, S. Ferrer, J. Borras, A. Castineiras, E. Monzani, L. Casella, *Inorg. Chem.* 2004, **43**, 6805.

5S. A. Granata, E. Monzani, L. Casella, *J. Biol. Inorg. Chem.* 2004, **9**, 903.

6S. R. P. Bonomo, V. Bruno, E. Conte, G. De Guidi, D. La Mendola, G. Maccarrone, F. Nicoletti, E. Rizzarelli, S. Sortino, G. Vecchio, *Dalton Trans*., 2003, 4406.

7S. The solubilization of potassium salts by complexation of $KO_2$ with crown ethers was reported in: (a) C. J. Pederson, *J. Am. Chem. Soc.*, 1967, **69**, 7017; (b) C. J. Pederson and H. K. Frensdorff, *Angew. Chem., int. Ed. Engl.*, 1972, **11**, 16; (c) J. S. Valentine, A. B. Curtis, *J. Am. Chem. Soc.* 1975, **97**, 224.

8S. B. H. J. Blelski, G. G. Shive, S. Bajuk, *J. Phys. Chem.* **1980**, 84, 830-833.